SPECTROPHOTOMETRIC PROPERTIES OF MERCURY'S SURFACE DERIVED FROM THE MESSENGER MASCS OBSERVATIONS. D. L. Domingue,[1] Mario D'Amore,[2] Sabrina Ferrari,[2] Jörn Helbert[2], and Noam R. Izenberg[3], [1](domingue@psi.edu) Planetary Science Institute 1700 E. Fort Lowell, Suite 106, Tucson AZ, 85719, USA. [2]Institute for Planetary Research, DLR, Rutherfordstrasse 2, Berlin, Germany; [3]The Johns Hopkins University Applied Physics Laboratory, 11100 Johns Hopkins Road, Laurel, MD 20723, USA.

Introduction: While element composition across the surface of Mercury has been mapped based on the X-ray Spectrometer (XRS) and Gamma-ray Spectrometer (GRS) observations on board the MESSENGER spacecraft [1-9], mineral compositional determinations have remained more elusive. Izenberg et al. (2014) presented a global analysis of the Mercury Atmosphere and Surface Composition Spectrometer (MASCS) spectra in the range from 300 nm to 1450 nm showing little regional variations in the absolute reflectance with no mineralogically diagnostic absorption features. The absorption band centered near 1 μm, diagnostic of ferrous iron in silicates, is not observed in the MASCS surface spectra, though there is evidence for a possible oxygen-metal charge transfer (OMCT) ultraviolet absorption consistent with an upper limit of ~1.8 wt% FeO that is observed in spectral ratios of bright unit (fresh craters and hollows) spectra with the average Mercury spectrum [10]. Further examination of the MASCS spectra show no absorptions diagnostic of sulfide minerals [10]; however, examination of color observations from the Mercury Dual Imaging System (MDIS) of craters containing hollows regions shows broad color signatures consistent with the presence of MgS [11]. These signatures are seen at a higher spatial resolution than possible with the MASCS observations, indicating the presence of this material is spatially variable and masked when mixed with other Mercury units [11]. In addition, despite the strong evidence of water ice in permanently shadowed regions [12], there is no evidence to date for hydroxylated materials near these regions [10].

Despite this lack of evidence for specific minerals across Mercury's surface, it is still informative to examine the spectral variability, especially as a function of geomorphological regions. Variations in spectral slope and absolute albedo can indicate variations in mineralogy, such as variations in the presence of opaques and glasses. In order to make these comparisons the variations due to illumination and viewing geometries (commonly referred to as photometry) need to be removed. To date the standardization to a common set of photometric angles has been performed using a simple Lommel-Seeliger and phase function correction. This empirical correction is independent of wavelength and therefore does not account for any possible spectral variations in photometric behavior. The Lommel-Seeliger function, which is a component of the empirical correction, does not account for possible variations in reflectance behavior with phase angle, and has been shown to perform worse at larger phase angles [13]. This is compensated for in the empirical correction with the use of a simple phase function [10].

A purpose of this study is to analyze a set of MASCS photometric observations and apply both the Hapke and Kaasalainen-Shkuratov models to examine if either can provide a more robust photometric correction to the MASCS spectra than the current empirical correction, and thus enable more refined comparisons of MASCS spectra across Mercury's surface. The MASCS data presented in this study is used to examine both the global and geomorphological variations in the photometric behavior of Mercury's surface.

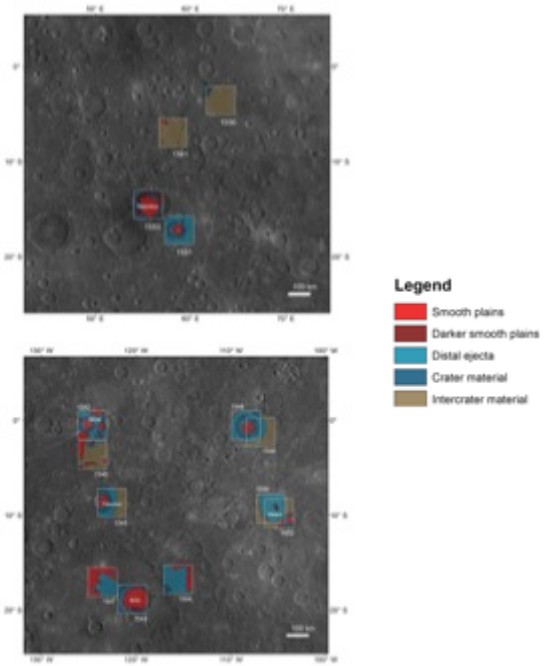

Figure 1. The MASCS photometric regions are identified in context with the surrounding geology from the MDIS monochrome mosaic. The eastern (top) and western (bottom) regions are plotted to show their location on the surface and the different geomorphological units present within each region is mapped. The numbers of each unit refer to their identifier in the photometric target data retrieval sequences.

Data Set: MESSENGER flew by Mercury three times (January 24, 2008, October 6, 2008, September 29, 2009) which provided a preview of the observations to come during the mission's orbital phase. Based on the flyby observations acquired by the Mercury

Dual Imaging System (MDIS), a set of regions for photometric characterization of the MASCS Visible and InfraRed Spectrograph (VIRS) data were defined based on their "generic" properties: (1) moderate albedo in the MDIS images, (2) no large basin or basin-like features, and (3) dominated by plains units. Selection of regions for photometric characterization was also based on the available range of incidence and emission angles at which the region could be observed while under the spacecraft operational constraints (the MASCS instrument was mounted on the spacecraft's instrument deck at a fixed 90° angle to the sun shield. MASCS observations were limited to 90° ± 12° in phase angle; this represents the allowable range within the spacecraft pitch and roll operations that would keep instrumentation and equipment safe behind the sun shield.) These criteria limited the regions to the southern hemisphere. The selected photometric regions and their geomorphological characteristics are shown in **Figure 1**. Note that these regions were selected based on the lower spatial resolution flyby data and the orbital data have now shown that the geomorphological assessment of these regions is anything but "generic".

The Models: Three models were examined and applied to the MASCS photometry data set: the current model used by the project for providing photometric standardization of the MASCS spectral data set, the Hapke Basic Model, and the Kaasalainen-Shkuratov (KS) model used to photometrically standardize the Mercury Dual Imaging System (MDIS) data. The current function used is given by: $f(i,e,\alpha)=(\cos i/(\cos i+\cos e))(0.0576 - 0.000352\alpha)$, where i, e, and α are the incidence, emission, and phase angles, respectively.

The Hapke Basic model is expressed as:

$$r(i,e,\alpha)=(w/4\pi)(\mu_{0e}/(\mu_{0e}+\mu_e)\{[p(\alpha)[1+B_{s0}B_s(\alpha)]] +H(\mu_{0e})H(\mu_e) - 1]\}S(i,e,a,\theta)$$

where w is the single scattering albedo, μ_{0e} and μ_e, are the cosines of the incidence (i) and emission (e) angles modified for surface roughness (see Hapke 1984, equations 46 – 50), respectively, α is the phase angle, $p(\alpha)$ is the single-particle scattering function, B_{S0} is the shadow-hiding opposition effect (SHOE) amplitude and the SHOE term B_S is given by:

$$B_s(\alpha)=[1+(1/h_s)\tan(\alpha/2)]^2$$

where h_s is the angular half-width of the SHOE peak (in radians). There are no observations with in the opposition region in the MASCS/VIRS data set, thus the values for B_{S0} and h_s are set to the values used by Domingue et al. (2016) [14], 3.086 and 0.090, respectively.

The KS model is given by:

$$KS=A_N e^{-\alpha\mu}[c_l(2\cos i/(\cos i+c\cos e))+(1-c_l)\cos i]$$

where KS is the predicted reflectance, A_n is the normal albedo, μ is related to the surface roughness, and c_l is the partition factor between Lommel-Seeliger (2cosi/(cosi+cose)) and Lambert (*cosi*) type scattering

Results: Modeling results between the Hapke and KS models show similar properties, and fit the data with similar robustness. Both of these models describe the data better than the current function in use by the project. Preliminary examination of updates to the coefficients in this function show that the Hapke and KS models still provide a moderately better prediction of the Mercury's surface reflectance.

For analysis purposes the data set divided into 3 categories: Category-1 data includes measurements from all the photometric regions regardless of geomorphological unit. Category-2 data segregates the data by geomorphological unit, but not region. Category-3 data segregates the data by region and by geomorphological unit. Modeling of each data set provides a method for examining the photometric variability across Mercury's surface and within similar geologic units and comparisons with its global properties. Preliminary examination indicates that the many of the variations are within the error limits of the parameters.

References: [1] Nittler et al. 2011, Science 333, 1847–1850, doi:10.1126/science.1211567 [2] Weider et al. 2012, J. Geophys. Res. 117, E00L05, doi:10.1029/2012JE004 [3] Weider et al. 2014, Icarus, 235, 170-186 [4] Weider et al. 2015, Earth and Planetary Science Letters, 416, 109-120 [5] Peplowski et al. 2014, Icarus, 228, 86-95 [6] Peplowski et al. 2015, Icarus, 253, 346-363 [7] Peplowski et al. 2015, Planetary and Space Science, 108, 98-107 [8] Evans et al. 2012, J. Geophys. Res. 117, E00L07, doi:101029/2012JE004178 [9] Evans et al. 2015, *Icarus, 257*, 417-427 [10] Izenberg et al. 2014, Icarus, 228, 364-374 [11] Vilas et al. 2016, Geophys. Res. Lett. 43, Issue 4, 1450 – 1456 [12] Lawrence et al. 2013, Science 339, 292–296, doi:10.1126/science.1229953. [13] Schröder et al. 2014, Planet. Space Sci. 103, 66-81. [14] Domingue et al. 2016, Icarus 268, 172 – 203